Solea senegalensis skeletal ossification and gene expression patterns during metamorphosis provide new clues on the onset of skeletal deformities.

Ignacio Fernández[1]*, Luis Granadeiro[1], Maria Darias[2], Paulo J. Gavaia[1], Karl B. Andree[3] and Enric Gisbert[3]

[1] *Centro de Ciências do Mar (CCMAR), Universidade do Algarve, Campus de Gambelas, 8005-139 Faro (Portugal)*

[2] *Institut de Recherche pour le Développement (IRD), Unité Mixte de Recherche Biologie des Organismes et Ecosystèmes Aquatiques (UMR BOREA – MNHN, CNRS-7208, UPMC, IRD-207, UCN, UA) 911 Avenue Agropolis, BP 64501, 34394 Montpellier Cedex 5, France*

[3] *IRTA, Centre de Sant Carles de la Ràpita (IRTA-SCR), Unitat de Cultius Experimentals, Crta. del Poble Nou s/n, 43540 Sant Carles de la Ràpita (Spain)*

[*] Corresponding author: Ignacio Fernández, *Centro de Ciências do Mar (CCMAR), Universidade do Algarve, Campus de Gambelas, 8005-139 Faro (Portugal)*. Tel.: +34 977745427; Fax: +34 977443138; E-mail: nacfm@hotmail.com; ivmonzon@ualg.pt; Web address: http://www.bioskel.ccmar.ualg.pt/

Abstract:

Farmed Senegalese sole (*Solea senegalensis*) still show a high incidence of vertebral anomalies that limit its intensive production and hamper its economic profitability. A great effort on the understanding how this fish species is developed and grows in captivity has been obtained in the last decade, and particularly how different biotic and abiotic factors affect its skeletal development. Although some work has been performed on its skeletal development and gene expression patterns of key developmental signaling pathways, a detailed description of the above-mentioned processes is still lacking. Here, the progression of skeletal development of cranial, appendicular and axial skeleton is provided through the implementation of an acid free double staining protocol; while the gene expression pattern of vitamin A (VA) and thyroid hormones (THs) signaling pathways through quantitative PCR (qPCR) has been performed along larval fish development under a standard larval rearing protocol. Moreover, the disruption of their gene expression patterns has been evaluated in Senegalese sole larvae fed with increased dietary VA levels (8-fold increase) during the *Artemia* feeding phase (from 6 to 27 dph). These results have been correlated with the prevalence of particular abnormalities in specific skeletal structures. While the ontogenetic study allowed us to identify the onset of the most common skeletal deformities affecting Senegalese sole rearing - the caudal fin vertebrae - and revealed a highly coordinated expression of VA- and TH-related genes; comparative gene expression analysis in larvae fed control and high dietary VA content identified the specific timing of VA and THs signaling disruption through which VA, and indirectly the THs, increased the incidence of skeletal deformities in this species. Present research work represent an important step forward towards the proper identification of the onset of skeletal deformities and urge the investigation of nutritional and rearing conditions during the switch of larval behavior - from pelagic to benthonic - in order to overcome skeletal deformities in an important southwestern Europe aquaculture fish species.

Keywords: flatfish; skeletogenesis; ossification; expression patterns; vitamin A; thyroid hormones; metamorphosis

1. Introduction

Skeletal deformities and, to a lesser extent, pigmentary disorders are two important factors reducing the productivity and profitability of farmed fish (Koumoundouros 2010; Boglione et al. 2013), and particularly that of Senegalese sole (Fernández & Gisbert 2011). At hatcheries, grading out malformed fish increase production costs. In on-growing farms, abnormal fish reaching the market size should be commercialized at a lower value or discarded. Furthermore, some skeletal anomalies might reduce feed conversion, growth potential, welfare and survival rate (Koumoundouros, 2010). However, despite the great effort in the last decades to identify the different (nutritional, environmental, and genetic) factors responsible for the appearance of skeletal anomalies in fish species, a consequent reduction on its incidence has been not achieved so far (Boglione et al. 2013; Ortiz-Delgado et al., 2014). The late detection of the problem (mainly at juvenile or adult stage), the uncertainty on the onset of the deformity, a lack of a clear etiology with a potential multifactorial cause and/or the absence of implemented and reliable early detection procedures at industrial level are different factors that may account for the still high incidence of abnormal skeletogenesis in farmed fish. For instance, while an external evaluation of Senegalese sole juveniles aged 255-352 days by fish farm staff revealed 16% of fish showing deformities, a radiographic study showed that indeed 78% exhibited malformations, while 20% exhibited severe deformities (Losada et al., 2014). The prevalence of skeletal abnormalities is highly variable, depending the body region affected, the severity, the species, the rearing system, the farm, and/or the batch of eggs (Boglione et al., 2013). In Senegalese sole, a high incidence of skeletal has been extensively found, reaching up to 90% of prevalence (Gavaia et al., 2002, 2009; Fernandez et al., 2009; Fernandez and Gisbert, 2010; Boglino et al., 2012; Dionísio et al., 2012; Losada et al., 2014; Richard et al., 2014; de Azevedo et al., 2017); being mainly located in the caudal region and comprising moderate to severe deformities of vertebral column, from flattened to trapezoidal vertebrae (Fernandez et al., 2009; Losada et al., 2014; Richard et al., 2014; Cardeira et al., 2015; de Azevedo et al., 2017).

Skeletogenesis is a key morphogenetic event in the embryonic and post-embryonic development of vertebrates by which the skeletal structures are formed. Different cell types, mainly chondrocytes, osteoblasts, osteocytes and osteoclasts, form cartilaginous and bone structures that constitute the skeleton (reviewed in Hall 2015). Skeletal structures may be formed by two distinct ossification processes, by chondral ossification, where a previously formed cartilage template is replaced by bone, and dermal or intramembranous ossification, where the bone is formed without a cartilage anlagen. Detailed knowledge on fish skeletal development and their underlying pathways is essential to understand how different factors might have an impact on it and thus, basic to identify and implement optimal rearing conditions in order to avoid the appearance of skeletal anomalies (Bird and Mabee 2003; Sæle et al., 2017). A limited information on Senegalese sole skeletal development is available, and restricted to the skeletal structures from the axial skeleton (Gavaia et al., 2002). In contrast, a detailed information is available on Senegalese sole organogenesis (Padrós et al., 2011), metamorphosis (Fernández-Díaz et al., 2001) and its control by THs (Manchado et al., 2008a, 2008b; Fernández et al., 2017).

Since marine fish hatch at a much earlier developmental stage than other vertebrates, nutrition, among other factors, plays a key role in controlling early fish development (Hamre et al., 2013; Pittman et al., 2013). In this regard, several nutrients have been linked a key role in determining skeletal phenotype when their level and/or form of supply in the diet were inappropriate or unbalanced (Boglione et al., 2013). Vitamin A (VA), a fat soluble vitamin that is not *de novo* synthesized by vertebrates (Ross et al., 2000), is one of the most extensively studied nutrients is this regard. Fish larvae fed high levels of VA showed an abnormal skeletogenesis (Fernández and Gisbert, 2011), being suggested that VA requirements are cell/tissue, developmental stage and species-specific dependent (Mazurais et al., 2009; Fernández et al., 2014). VA signaling is controlled by retinoic acid receptors (RARs: α,β,γ) and retinoid X receptors (RXRs: α,β,γ; Henning et al., 2015). Early mechanistic approaches to unveil which specific signaling pathway driving skeletogenic phenotype in fish species proposed the alteration of RARs (Haga et al., 2003) or more specifically RARγ and RXRα (Villeneuve et al., 2006) as the main responsible ones. More recently, *in vivo* and *in vitro* studies have suggested the disruption of RARα as the main VA nuclear receptor controlling skeletal development under dietary VA imbalance (Fernandez et al., 2011, 2014). Among different endocrine factors, the thyroid hormones (THs) are known to play a key role on bone development (Gogakos et al., 2010) and fish metamorphosis (Manchado et al., 2008a, 2008b; Gomes et al., 2015; Shao et al., 2016). Previous results showed how a dietary VA excess during the *Artemia* feeding phase affected the number and size of thyroid follicles as well as the TH immunoreactivity during Senegalese sole metamorphosis (Fernández et al., 2009). More recently, we demonstrated how VA affects Senegalese sole development in a TH signaling and metamorphic stage dependent manner (Fernández et al., 2017). Additionally, exposure to RA signaling agonist and antagonist disrupted THs signaling (Boglino et al., 2016). In this sense, although the gene expression profile of TH signaling have been previously studied during the metamorphosis in Senegalese sole (Manchado et al., 2008a, 2008b); how VA and TH signaling might be correlated with ossification during metamorphosis remains to be uncover.

The present research work, aimed to provide new insights on (i) the development of the whole skeleton and its ossification pattern along metamorphosis in Senegalese sole; (ii) how the above-mentioned process is correlated with gene expression patterns of VA and TH signaling pathways; and (iii) which are the main underlying pathways disrupted under a dietary VA excess that lead to skeletal deformities.

2. Materials and methods

2.1. Ethics statement

All experiments were performed according to 2010/63/EU of the European Parliament and Council and the related guidelines (European Commission, 2014) for animal experimentation and welfare. Animal experimental procedures were conducted in compliance with the experimental research protocol (reference number 4978-T9900002) approved by the Committee of Ethic and Animal Experimentation of the IRTA and the Departament de Medi Ambient i Habitatge (DMAH, Generalitat de Catalunya, Spain). For sampling purposes, soles were sacrificed with an overdose of anesthetic (Tricaine methanesulfonate, MS-222, Sigma-Aldrich).

2.2. Standard larval rearing and sampling

Newly hatched larvae were distributed (initial density: 80 larvae L^{-1}) in 2 cylindrical tanks (500 L) connected to a recirculation unit (IRTAmar™). Water conditions were as follows: 18.0 ± 1.0 °C, 35 ppt salinity, pH between 7.8 and 8.2, and daily exchange of water (20%) in the recirculation system with gentle aeration and oxygenation (>4 mg L^{-1}). Photoperiod was 12 L:12 D and light intensity was 500 lx at water surface.

General feeding protocol for Senegalese sole used in the present study was as follows: pre-metamorphic larvae were fed from 3 days post hatch (dph) to 10 dph with rotifers (*Brachionus plicatilis*) enriched with Easy Selco™ (ES, INVE, Belgium). Rotifer density in larval rearing tanks was 10 rotifers mL^{-1} from 3 to 6 dph and it was gradually reduced to 5 rotifers mL^{-1} at 10 dph. Rotifer density was adjusted twice a day in order to assure the optimal prey density. Enriched *Artemia* metanauplii (EG, INVE, Belgium) were offered to sole from 6 to 40 dph at increasing densities from 0.5 to 12 metanauplii mL^{-1}. *Artemia* metanauplii density was adjusted four times per day (at 9, 12, 15 and 18 h) to assure the optimal prey density and nutritional VA value, as described in Cañavate et al. (2006). From 20 dph onwards, when individuals showed a complete eye migration and start to show a benthonic behavior, the volume of rearing tanks was reduced and enriched *Artemia* was delivered frozen. Both live preys were enriched as previously described in Fernández et al. (2008). From 41 dph to the end of the experiment (55 dph), post-metamorphic larvae were weaned onto dry feed (Gemma Micro 150–300© Skretting, Spain).

2.3. *Larval rearing under dietary VA imbalance*

A second trial was conducted to evaluate the effects of VA imbalance on sole skeletogenesis and VA and TH signaling pathways. Thus, newly hatched larvae were distributed (initial density: 80 larvae L^{-1}) in 21 cylindrical tanks (100 L) connected to a recirculation unit (IRTAmar™), and under the same environmental and feeding regime conditions previously described for the standard larval rearing.

The effect of VA in Senegalese sole larval performance and skeletogenesis was previously evaluated by means of four different dietary regimes containing graded levels of VA and using enriched *Artemia* metanauplii as carrier; each regime was done in triplicate (Fernández et al., 2009). In brief, graded levels of VA in *Artemia* metanauplii were obtained by adding different amounts of retinyl palmitate (1,600,000 IU g−1, Sigma-Aldrich, Spain) to a commercial enriching emulsion (Easy Selco™, INVE, Belgium). Here, expression levels of genes playing a key role in skeletogenesis, VA and thyroid metabolism and signaling were evaluated in fish fed *Artemia* enriched with the Control (1.32 ± 0.03 μg total VA mg^{-1} DW; Control group) or highly supplemented VA (12.91 ± 0.06 μg total VA mg^{-1} DW; VA group) emulsion, formerly D1 and D4 experimental groups in Fernández et al. (2009).

2.4. *Sampling and growth analysis*

At 2, 5, 9, 13, 21, 30 and 45 dph, soles under standard larval rearing protocol were sampled for growth in standard length (SL) and skeletal development. At each sampling time, 10 specimens were randomly sampled, anaesthetized and SL determined using a digital camera connected to a binocular microscope Nikon SMZ 800 and an image analysis system (AnalySIS, Soft Imaging Systems, GmbH). Once larvae were measured in SL, they were sacrificed with an overdose of MS-222, rinsed in distilled water and fixed in 4% buffered (pH 7.4) formaldehyde and stored at 4 ºC until the skeletal analysis.

At 10, 15, 30 and 45 dph, Control and VA groups from the dietary VA imbalance trial were sampled for survival, growth, retinoid content, and skeletal development analysis as reported in Fernández et al. (2009).

2.5. Skeletal development analysis

To evaluate the mineralization degree of the skeleton, and to identify and quantify the incidence of skeletal deformities, animals were stained for bone and cartilage in whole mount preparations using an optimized acid-free staining protocol from Walker and Kimmel (2007) in samples from 2 to 13 dph in order to avoid loss of calcium in incipient ossified structures. An acid staining method (Klymkowsky and Hanken, 1991) in later samplings was used to warrant sufficient penetration of dyes on fish body. Skeletal structures were identified and named according to Okada et al. (2001), Wagemans and Vandewalle (2001) and Gavaia et al. (2002). The development of skeletal structures was categorized as cartilaginous, on its onset of ossification and with advanced ossification (when almost all the structure is ossified).

2.6. Gene expression analysis

For gene expression analysis, pools of fish (50 to 3 individuals per sample, depending on their size) were sacrificed with an overdose of MS-222, rinsed in distilled water, frozen stored at –80 ºC in TRIzol reagent (Invitrogen®, San Diego, CA, USA) until total RNA was extracted. Samples were taken at 5, 9, 13, 14, 16, 19, 21, 30 and 45 dph during the standard larval rearing, while at 10, 15, 30 and 45 dph from Control and VA fed larvae from the dietary VA imbalance trial.

Gene expression patterns of nuclear receptors for VA and TH, their signaling as well as for the bone Gla protein encoding genes during larval development, but also under different VA dietary regimes (Control *versus* VA) were evaluated. In both experiments, total RNA was extracted using the TRIzol reagent as specified by the manufacturer. RNA was quantified using a Gene-Quant spectrophotometer (Amersham Biosciences) and purity established by the absorbance ratio 260/280 nm. The integrity of the RNA was examined by gel electrophoresis. Total RNA (1 µg) was retrotranscribed using the QuantiTect Reverse Transcription Kit (Qiagen®); electrophoresis using a 1.2% agarose gel was run to assess the specificity of RT-PCR product. Real-time qPCR was performed using an ABI PRISM 7300 (Applied Biosystems). For each gene, a species-specific Taqman assay was designed (Applied Biosystems) using the sequences acquired from the GenBank database (Table 1). The efficiency of the Taqman assay for each gene was previously evaluated to assure that it was close to 100%. All reactions were performed in 96 well plates in triplicate in 20 µl reaction volumes containing: 10 µl of 2× TaqMan universal PCR master mix (Applied Biosystems); 1 µl of the 20× Taqman primer/probe solution corresponding to the analyzed gene; 8 µl of molecular biology grade water; and 1 µl of cDNA diluted 1:10, with the exception of *bone Gla protein* (*bgp*), which was evaluated with a 1:5 dilution. Standard amplification parameters were as follows: 95 °C for 10 min, followed by 45 amplification cycles, each of which comprised 95 °C for 15 s and 60 °C for 1 min. Real time qPCR was performed for each gene following MIQE guidelines such as including a calibrator sample within each plate (Bustin et al., 2009). The relative gene expression ratio for each gene was calculated according to Pfaffl (2001). Relative gene expression was normalized using *ubiquitin* (UBQ), a previously reported reference gene for accurate normalization in qPCR studies with Senegalese sole (Infante et al., 2008; Richard et al., 2014; Fernández et al., 2015). Reference samples were the 9 dph and Control group from the standard and the VA imbalance trials (respectively), and set to 1.

2.7. Statistical analysis

Results are given as mean and standard deviation. All data were checked for normality (Kolmogorov–Smirnov test) and homoscedasticity of variance (Bartlett's test). Gene expression ratios along Senegalese sole development (standard larval rearing) were compared by means of One Way ANOVA. When significant differences were detected, the Tukey multiple-comparison test was used to detect differences among experimental groups. Data from dietary VA imbalance trial was compared by a Student t-test. The level of significant difference was set at $P < 0.05$. All the statistical analyses were conducted using GraphPad Prism 5.0 (GraphPad Software, Inc.).

3. Results

3.1. Skeletal development and ossification pattern

Skeletal development of Senegalese sole along metamorphosis was evaluated in the cranial (Fig. 1), trunk (Fig. 2) and caudal (Fig. 3) regions. At 2 dph, the first cartilaginous structures observed were the Meckel's cartilage, the ethmoid and the pectoral fin. At 5 dph, the anguloarticular, hyoid, quadrate, interhyal, hyomandibular and ceratobranchials were also present as cartilaginuous structures, while the cleithrum structure was identified with an incipient ossification (Supplementary Fig. 1a). Between 5 and 9 dph, other cranial structures were developed such as the maxillary, pre-maxillar, ectopterygoid, preopercular and the parasphenoid (Supplementary Fig. 1b). All those previously described structures (with the exception of the ones composing the pectoral fin) reached an advanced ossification at the beginning of the pre-metamorphosis (9 dph). At this stage, the intramembranous structure exoccipital from the cranial region and dorsal and ventral rays, cephalic, abdominal and caudal vertebrae (1-12) from the trunk started to ossify. Concomitantly, neural spines from first (cephalic) to 20th (caudal) vertebrae and haemal spines (1-12), as well as parapophysis 6 to 8 initiated their ossification. Such parallel ossification process observed between vertebrae and their correspondent neural and haemal spines was not observed in posterior vertebrae. In this sense, while caudal vertebrae 13-21 begun to show mineralization between 9 and 13 dph, and caudal vertebrae 22-29 at 13 dph, their correspondent neural and haemal spines already showed it at 9 dph and between 9 and 13 dph, respectively. At the caudal region, first structures started to develop at 9 dph as a cartilaginous anlagen (hypurals 1-4 and parahypural), while fin rays initiated their ossification as intramembranous structures. Just before pro-metamorphosis taking place (between 9 and 13 dph), caudal vertebrae 13-21 exhibited incipient mineralization, as well as neural and haemal spines from the future caudal vertebrae 28-29.

At the onset of pro-metamorphosis (Supplementary Fig. 1c), in the cranial skeleton, supraorbital canal bones, the frontal, supraoccipital, epioccipital, pterotic and sphenotic bones showed the first ossification signs; while the exoccipital had an advanced level of ossification. In the trunk, structures (cartilaginous) from the pelvic fin were formed, whereas an advanced ossification in the different structures composing the whole vertebral column (vertebrae, neural and haemal spines) was progressively revealed. Cephalic, abdominal and caudal vertebrae up to the 21^{st} and their respective neural spines ossified. While parapophysis 4-5 begun to be mineralized, haemal spines 1-29 had already mineralized. Caudal vertebrae 22-34 initiated their mineralization, as well as 38-42 neural and 30-34 haemal spines. At this time, the neural spine 44 and haemal spine 35 started to be formed through a chondral ossification process, in contrast to the rest of haemal and neural elements; while the urostyle showed an incipient mineralization. A progressive development on the caudal fin elements was evidenced too. In this sense, modified neural and haemal spines, the epural and hypural 5 were present, although still in a cartilaginous state. Hypurals 1-4 started to ossify, while fin rays already showed extended ossification.

At the end of the pro-metamorphic stage (21 dph), no further progression on the formation and ossification of the cranial structures was evidenced, unless the starting ossification of the lateral ethmoid. In contrast, the ossification process was almost finalized on the trunk where all the structures showed an extended ossification state with the exception of parapophysis 4-5, the dorsal and ventral pterigophores, as well as the skeletal structures from the pelvic and pectoral fins. Similarly, all caudal fin structures showed an advanced level of ossification at this stage.

At post-metamorphosis (Supplementary Fig. 1d), all elements from the cranial skeleton showed an advanced stage of ossification with just three exceptions. The mesethmoid and sphenoid that started to mineralize at 30 dph, showing full mineralization at 45 dph when the lateral ethmoid also completed its ossification. In the trunk, the elements that were not already fully ossified (dorsal and ventral pterigophores, pelvic and pectoral fin structures and parapophysis 4-5) completed their ossification at 30 dph.

A specific ossification pattern in Senegalese sole was finally revealed when representing the metamorphic stage at which an advanced level of mineralization in each skeletal structure was achieved (Fig. 4). While elements involved in breathing and feeding processes were already ossified during the pre-metamorphic stage (2-9 dph), axial skeleton was almost completed at pro-metamorphosis (9-21 dph). Only structures involved in the eye migration process showed extended ossification at post-metamorphosis (>30 dph).

3.2 Gene expression patterns of VA and THs signaling pathways along metamorphosis

The expression of *retinoic acid receptor α* (*rarα*), *retinoid X receptor α* (*rxrα*) and *retinol binding protein* (*rbp*); *thyroid hormone receptor α A* (*trαa*), *thyroid hormone receptor α B* (*trαb*), *thyroid hormone receptor β* (*trβ*), *thyroglobulin* (*tg*) and *thyroid stimulating hormone β* (*tshβ*); and *bone Gla protein* (*bgp*), representatives of the VA and THs signaling pathways and bone ossification, respectively; is presented in Figure 5. The expression of *rarα* increased from 5 dph until 14 dph when reached a peak in expression (2.60 ± 0.02 relative expression units (REU)), but decreasing afterwards showing low expression values at 21 dph (end of pro-metamorphosis; 1.06 ± 0.13 REU). From this stage onwards, the expression of *rarα* increased again and remained constant until the end of the trial (45 dph; 2.01 ± 0.14 REU). The profile of *rxrα* along Senegalese sole metamorphosis was similar to that of *rarα*, showing high values during the climax of metamorphosis (13-16 dph; increasing from 1.98 ± 0.57 to 2.26 ± 0.08 REU). In the case of *rbp*, its expression was highest at 13 dph (1.70 ± 0.14 REU) and lowest at 5 and 21 dph (0.36 ± 0.01 and 0.52 ± 0.06 REU, respectively).

Regarding the THs signaling pathway, both *trαa* and *trαb* showed almost equal gene expression profiles along fish metamorphosis, and similar to those of *rxrα.* From 5 dph, transcript levels increased onwards, reaching their highest values at 13-16 dph (values ranging between 1.69 ± 0.12 and 2.19 ± 0.19 REU), but shortly after decreasing at 19 dph (0.73 ± 0.43 REU in *trαa* and 0.93 ± 0.12 REU in *trαb*) and remaining low until the end of the trial. In contrast to what was found in *trα* isoforms, *trβ* exhibited a sharp increase during the first part of pro-metamorphosis (from 0.94 ± 0.12 at 9 dph to 4.72 ± 0.06 REU at 14 dph), decreasing a little until 21 dph (2.86 ± 0.26 REU) to increase again afterwards (5.21 ± 0.25 to 5.52 ± 0.02 REU). The gene expression profile of *tshβ* during larval development was somehow flat, although a slightly higher value was observed at 9 dph (1.15 ± 0.18 REU); while the one of *tg* showed again an increased expression from 5 dph (0.15 ± 0.01 REU) till 19 dph (4.25 ± 0.03 REU), and remaining low afterwards.

Opposed to the previously described gene expression patterns, *bgp* expression was not detected at 5 dph and tend to increase along larval development, reaching a 187.85-249.65 REU at the end of the pro-metamorphosis (19-21 dph), although a significant and sharp increase was found at 30 dph (1061.95 ± 195.85 REU).

3.3 Gene expression disruption under dietary VA imbalance

Under dietary VA imbalance, Senegalese sole larvae only showed a disruption on gene expression of particular genes during specific developmental stages. At 10 dph, only the expression of *rarα* and *tg* genes was significantly altered in sole fed high dietary VA levels when compared to those fed the control diet, being both genes down-regulated (expression varied from 0.88 ± 0.04 to 0.75 ± 0.03 and from 1.05 ± 0.07 to 0.27 ± 0.03, respectively; Fig. 6a). A higher effect in gene expression was observed in soles during pro-metamorphosis (15 dph) when fed with high dietary VA levels (Fig. 6b). In this sense, gene expression of *rarα*, *rxrα*, *trαa*, *trαb* and *bgp* was found to be up-regulated (values ranging from 1.63 ± 0.06 to 2.13 ± 0.11 REU) respect to that of the Control group. In contrast, during post-metamorphosis, only *bgp* still showed significantly increased gene expression levels in fish fed high dietary VA content (1.47 ± 0.23 and 2.73 ± 0.82 REU at 30 and 41 dph, respectively; Fig. 7).

4. Discussion

Overcoming aquaculture bottlenecks requires the definition and implementation of early detection systems and quality indicators, allowing in the particular case of skeletal deformities to identify the precise time of their onset and a better characterization of their etiology (Boglione et al., 2013). Furthermore, for unveiling the etiology of an abnormal output in production traits the understanding of their underlying mechanism has been recognized as a key issue (Manchado and Cerda, 2013). In this sense, basic knowledge on the normal course of skeletal development, as well as their mechanisms at molecular level is essential in fish biology (Bird and Mabee, 2003), particularly to reduce (if not totally avoiding) the appearance and the severity of skeletal deformities in fry. Since fish is one of the most evolved and diverse taxonomic groups, showing a wide diverse range of phenotypes/morphologies, the study of the ontogenetic (skeletal) development for each species is required. Furthermore, since developmental changes and sequences are specifically linked to particular genetic, and thus, transcriptomic changes (Liu et al., 2015), the characterization of the normal gene expression profiles and its disruption by environmental or biotic factors should be a priority.

4.1 New insights on the standard developmental sequence of Senegalese sole skeleton

Previous studies have already described the chronological development of the axial skeleton in Senegalese sole along larval development (Gavaia et al., 2002) although using a modified protocol of double staining technique acid solution (Gavaia et al., 2000), and not differing in the particular timings at which skeletal elements were cartilage, started to mineralize or fully mineralized. Similar procedures (with acid solution) have been already applied to study the skeletogenic development of different fish species. The development of the cranial skeleton of other flatfish species such as the common sole (*Solea solea*; Wagemans and Vandewalle, 2001), the Japanese flounder (*Paralichthys olivaceus*; Okada et al., 2003) and the Atlantic halibut (*Hippoglossus hippoglossus;* Sæle et al., 2004); the viscerocranial and axial skeleton of gilthead sea bream (*Sparus aurata*; Faustino and Power, 1998, 1999, 2001) or the zebrafish (*Danio rerio*) skeleton (Cubbage and Mabeee, 1996; Bird and Mabee, 2003) have been described using such acid staining protocol. The development of early bony ossification in fish species through an acid free double staining technique, and thus reducing of inaccuracies on skeletal development descriptions due to a decalcification of small structures undergoing ossification, was possible since 2007 where an optimized acid free double staining protocol was used to study zebrafish skeletogenesis (Walker and Kimmel, 2007). Instead, the skeletal development of Atlantic cod (*Gadus morhua*; Sæle et al., 2017) has been recently described using only alizarin red staining to avoid calcium phosphate removal during cartilage staining procedure. Nevertheless, several skeletal structures ossified through chondral ossification (endo- or peri-chondral) process are critical on larval viability (e.g. ethmoid and dentary, among others involved if the feeding apparatus) and being more prone to exhibit an abnormal development than those intramembranous under suboptimal rearing conditions (Fernandez and Gisbert, 2010). Thus, the accurate description of skeletal development of chondral and intramembranous structures might be a key issue to identify the timing and the causative factor of abnormal skeletogenesis.

While X-ray and computed tomography analysis allow a quick and clear diagnosis of skeletal deformities in fish juveniles/adults (Gisbert et al., 2012; Losada et al., 2014); present implementation of an acid free double staining protocol allowed us to simultaneously identify when first cartilaginous and bonny ossification appeared in Senegalese sole and how its skeletal development progressed. In the present work, first skeletal elements to be formed are those located in the cranial region, related with feeding (Meckel’s cartilage, ethmoid, angular, quadrate, hyoid, interhyal and hyomandibular in a cartilaginous form) or respiratory purposes (ceratobranchials in a cartilaginous form and cleithrum as bone structures. The progression of the ossification of these cranial structures has been revealed to occur fast, as most of them already showed an advanced ossification at 9 dph. This relative chronological order of ossification was similar to the previously reported pattern described in other fish species (Wagemans and Vandelle 2001; Faustino et al., 2001). In contrast, Senegalese sole skeletal elements forming the skull were found to be the latest to be fully ossified, similar to other fish species like Atlantic cod (Sæle et al., 2017), gilthead sea bream (Faustino and Power, 2001) or zebrafish (Cubbage and Mabeee, 1996). In sole, the late mineralization of the above-mentioned cranial structures during post-metamorphosis allowed the proper development of the brain, and cranial remodeling associated with eye migration process occurring during flatfish metamorphosis (Boglino et al., 2013).

The development of the axial skeleton in Senegalese sole was sequential and unidirectional, from the first cephalic vertebrae to the urostyle, similarly to the previous description of this fish species (Gavaia et al., 2002) and other fish species like Atlantic cod (Sæle et al., 2017), but differed from that of zebrafish or gilthead sea bream where ossification started at centra 3-4 and proceeded bidirectionally (Bird and Mabee, 2003; Faustino and Power 1998). The vertebral column, composed by vertebral centra, neural and haemal arches and spines, the parapophyses and the ventral ribs is formed by intramembranous ossification, with the exception of thee arches and spines of the preural centra, which calcify by endochondral ossification (Gavaia et al., 2002). Nevertheless, using an acid free staining we were able to report the first ossified vertebrae in larvae aged 9 dph (4.5 ± 0.29 mm SL), in contrast to previous description of the development of vertebral ossification in this species, where first ossified elements were found in 13 dph (4.3 mm SL; Gavaia et al., 2002). Those results evidenced the greater accuracy and relevance of use of the acid free double staining protocol for the proper ontogenetic description of fish skeletogenesis; although discrepancies can also be due to differences in fish size, since ossification stage is better correlated with fish size than with age (Sæle et al., 2017). The cephalic (1-3), the abdominal (1-5) and the most of caudal (1-21) vertebrae initiated ossification process at the end of pre-metamorphosis and were fully mineralized at pro-metamorphosis. The mineralization of caudal 22-35 and the preural (1-2) vertebrae started at pro-metamorphosis, whereas they were fully mineralized at the end of this developmental stage. Ontogenetic ossification of the axial skeleton might reflect the biological requirements of the species, allowing body flexibility at early life stages of development, being the notochord responsible for the proper posterior morphogenesis of the vertebral centra (Witten et al., 2005); as well as sustaining the musculature and allowing swimming activity afterwards. Senegalese sole metamorphosis from a pelagic to a benthonic behavior implies a change in swimming activity. Pre-metamorphic Senegalese sole larvae show a more constant and active swimming activity on the water column and a low body weight to sustain, while at the end of pro-metamorphosis swimming activity is occasional although vertebral column should sustain a higher body weight, particularly on the anterior part of the body. This might explain while last caudal vertebrae are only fully mineralized when Senegalese sole are settled. Moreover, this sequential ossification of vertebral column and swimming behavior has been hypothesized as being responsible of the higher skeletal deformity incidence in the axial skeleton on farmed Senegalese sole in comparison to other round fish species (Fernández, 2011). Interestingly, most skeletal deformities affecting Senegalese sole are located in these last vertebrae to ossify, which take place at the end of pro-metamorphosis. This developmental period is when larvae switch from pelagic to benthonic behavior, a stressful condition that might lead Senegalese sole to be more prone to abnormal skeletogenesis.

Similarly to the earlier ossification process of the axial skeleton in Senegalese sole unveiled herein, the development and ossification of the caudal fin complex has been found to occur earlier than previously described by Gavaia et al. (2002). While at 13 dph (4.3 mm SL) only hypurals 1 and 2 were observed and hypural 1-4 were present in the caudal fin complex at 15 dph (4.45 mm SL; Gavaia et al., 2002); in the present study, we were able to observe hypural 1-4, parahypural and fin rays in 9 dph larvae. Thus, although there is a large variation in size and stage of development of larvae of the same age in Senegal sole (Gavaia et al., 2002), present results using an acid free double staining protocol allowed us to perform a more accurate description of sole skeletogenesis.

4.2 Gene expression patterns of VA and THs signaling pathways along development are coordinated during Senegalese sole metamorphosis and their disruption linked to abnormal skeletogenesis

The VA and THs signaling pathways tightly control vertebrate's development (Ross et al., 2000; Gogakos et al., 2010). In fish and amphibians, THs signaling is largely known to drive metamorphosis process (Campinho et al., 2010; Gomes et al., 2015). While a crosstalk between VA and THs pathways in flatfish metamorphosis (eye migration and adult pigmentation acquisition) has been recently hypothesized (Shao et al., 2016); we previously showed an advanced eye migration process in Senegalese sole fed increasing levels of VA, probably related to the effect on thyroid follicles development and THs immunoreactiviness (Fernández et al., 2009). More recently, the interaction between both signaling pathways has been shown to be dose- and developmental time-dependent in Senegalese sole: the earlier the nutritional imbalance applied, the higher the effect on skeletogenesis (Fernández et al., 2017).

Since the regulation of the developmental processes involves the control of gene expression, deciphering the ontogenetic mechanisms and underlying regulations governing the harmonious development of larvae is essential to understand the disruptions induced by environmental and/or nutritional factors (Mazurais et al., 2012). In the present work, the gene expression patterns of VA and THs receptors and related genes (*rbp*, *tshβ*, *tg* and *bgp*) during Senegalese sole metamorphosis has been studied during normal and standard rearing conditions, as well as their regulation under hypervitaminosis A during the *Artemia* feeding phase.

The gene expression patterns of *rarα*, *rxrα*, *rbp*, *trα*, *trαb*, *trβ* and *tg* increased from hatching until the first part of pro-metamorphosis, decreased between the end of pro-metamorphosis and the beginning of post-metamorphosis, and increased again afterwards. Similar results have been previously reported in this species, regarding *trs* and *tg* (Manchado et al., 2008a; 2008b). Curiously, lowest gene expression was concomitant with the developmental phase where the completion of Senegalese sole organogenesis took place (end of pro-metamorphosis, Padrós et al., 2011), but when the ossification of the last caudal vertebrae and the preural vertebrae was still ongoing (present study). These gene expression patterns are in line with the reported roles of THs and VA in vertebrates (Ross et al., 2000), and more specifically in flatfish species (Gomes et al., 2015). *In vivo* and *in vitro* reports suggested the isoform *rara* as the most consistently disrupted VA receptor under dietary VA excess inducing skeletal deformities in fish species (Fernández et al., 2011, 2014); and main responsible of the developmental dependent dietary VA disruption of sole skeletogenesis (Fernández et al., 2017). The dietary VA excess in the present work - applied from 6 to 27 dph - induced a higher incidence of skeletal deformities, particularly on vertebrae and on the preopercular, interopercular, ceratohyal, and ceratobranchials 1–5 structures (Fernández et al., 2009). The developmental stage when the dietary VA imbalance was applied and the zone of the skeleton where deformities developed was somehow correlated, and particularly when dietary imbalance disrupted VA and THs signaling during pre- and pro-metamorphosis (larvae aged 10 and 15 dph; present study). Similarly, Senegalese sole fed dietary excess at particular defined developmental stages (pre-, pro- or post-metamorphosis) showed an increased mineralization degree only in the skeletal structures that were formed/mineralized in those particular developmental stages (Fernández et al., 2017). These results reinforced the idea of gene expression disruption of *rarα* during pre- and pro-metamorphosis being responsible for the higher incidence of vertebral deformities, which was in agreement with the key role of VA in vertebral segmentation (Haga et al., 2009; Laue et al., 2009), and cell proliferation, differentiation and mineralization processes in skeletal cells (Fernández et al., 2014).

The Senegalese sole has genes encoding for *trαa* and *trαb* isoforms in addition to the already-described *trβ* (Manchado et al., 2008a). A dietary VA imbalance (10 and 50 times higher) in enriching live prey emulsion only induced an increased expression of the different TRs isoforms in 6 dph pre-metamorphic sole larvae (Fernández et al., 2017). In the present study, larvae fed enriched *Artemia* with higher VA levels (8 fold increase) in the enriching emulsion exhibited an increased gene expression of *trαa* and *trαb* isoforms only in 10 dph larvae, whereas no disruption of *trβ* was found at any sampled time (age). Since a whole body RNA extraction was performed, and these receptors are ubiquitously expressed in Senegalese sole tissues (Manchado et al., 2008a); we cannot ascribe the altered gene expression of *trαa* and *trαb* isoforms to a specific tissue. Nevertheless, both TR isoforms are known to play an important role in bone morphogenesis (reviewed in Basset and Williams, 2016) and its disruption might be responsible, at least in part, of the skeletal deformities found in Senegalese sole larvae fed with increased levels of VA, and particularly those located in the caudal vertebrae found in Fernández et al. (2009, 2017).

The levels of THs are regulated through the pituitary–thyroid axis mainly by TSH and TG, among other factors (Pittman et al., 2013). Their role on TH synthesis in the thyroid follicle and its negative regulation by TH are well established in Senegalese sole (Manchado et al., 2008b). In Senegalese sole, gene expression of *tshβ* was already found to be up-regulated only during pre-metamorphosis when larvae were fed with extremely high levels of VA (50-fold increase) but not with moderate levels (10-fold increase), and neither during `pro- and post-metamorphosis regardless the dietary VA content applied (Fernández et al., 2017). In the present study, no differences in *tshβ* expression were found at any of the evaluated sampling times which might be due to the lower level of hypervitaminosis A applied [8-fold increase *versus* 50-fold increase in Fernandez et al. (2017)]. Regarding *tg*, a similar gene expression pattern has been previously described, with a sharply increase at the onset of metamorphosis, but decreasing after the climax of metamorphosis (Manchado et al., 2008b). TG is known to act as a matrix for thyroid hormone biosynthesis, being associated its impairment with abnormal TH biosynthesis (Targovnik et al., 2011). Thus, the present low *tg* expression levels found in larvae aged 10 dph fed high dietary VA content might be related with the increased number of thyroid follicles and the advanced eye migration stage previously reported in the same larvae (Fernández et al., 2009).

Finally, regarding skeletal mineralization, we have evaluated *bgp* (also known as *osteocalcin*) gene expression along larval development and under dietary VA excess. Although a broad range of whole-organism physiological roles have been recently attributed to *bgp* (Karsenty and Ferron 2012), it has been extensively described as a specific bone marker (Pinto et al. 2001), and is one of the most suitable biomarkers for skeletal development (reviewed in Cabrita et al., 2016). Similarly to Fernández et al. (2017), expression of *bgp* has been not detected at 10 dph (pre-metamorphosis). Increased levels were found at later stages, concomitantly with the increase in the level of skeletal mineralization already reported *in vivo* ((Gavaia et al., 2006; Fernández et al., 2011) and *in vitro* (Fernández et al., 2014) studies. In the present work, feeding dietary VA excess lead to an increased expression of *bgp* at 15, 30 and 41 dph. Contradictory results on the effect of a dietary/exposure VA increase on *bgp* gene expression were already reported: *in vivo* and *in vitro* up-regulation in gilthead sea bream (Fernández et al., 2011, 2014); *in vivo* down-regulation in Atlantic cod (Lie and Moren, 2012); and lack of gene expression disruption *in vivo* in Senegalese sole larvae (Fernández et al., 2017). The use of different approaches, VA imbalance and developmental stage applied might be account for these discrepancies.

Altogether, considering that farmed Senegalese sole is morphologically mostly characterized by showing a high incidence of skeletal deformities in caudal fin vertebrae (from 40 to 100%; Gavaia et al., 2002; Fernández et al., 2009, 2017; Dionísio et al., 2012; Losada et al., 2014; Richard et al., 2014; de Azevedo et al., 2017), and these vertebrae are formed during pro-metamorphosis and are fully mineralized at the end of this metamorphic phase; dietary VA content or other biotic or abiotic factor during this specific metamorphic phase seem to be the responsible of their abnormal development. Thus, further research effort should be conducted to investigate if other factors that are particularly changing during pro-metamorphosis like animal behavior (pelagic *versus* benthonic larvae) and the related environmental conditions (e.g. light exposure among others) might be the triggers of abnormal skeletogenesis in Senegalese sole.

5. Conclusions

The implementation at hatcheries and nurseries of more accurate diagnosis methods others than visual screening of the skeletal development has been recently recommended (de Azevedo et al., 2017). Nevertheless, little insights on the onset of skeletal deformities have been obtained. Here, an acid free double staining procedure allowed us to provide a more accurate and detailed description of the developmental timing at which the different skeletal structures were formed in Senegalese sole, and the described staging system might be used as a reference for future studies. Moreover, the comparative analysis of skeletogenesis with the externally easily to identify developmental stages (pre-, pro- and post-metamorphosis) showed that end of pro-metamorphosis seemed to be the onset of the abnormal development of the most affected skeletal structures in farmed Senegalese sole, the caudal fin vertebrae. In addition, a highly coordinated gene expression patterns of VA and THs signaling pathways with skeletal development and metamorphic stage was revealed, while its disruption at specific developmental times was correlated with skeletal deformities in particular structures (ceratobranchials and caudal fin vertebrae). While the implementation of such acid free staining on research studies towards rearing protocols improvements are recommended; the characterization and comparative analysis of VA and THs signaling pathways during development and dietary VA imbalance, further suggest to investigate nutritional regimes and rearing conditions and their relation with larval behavior switch (from pelagic to benthonic) in order to get clues on the triggers of caudal fin vertebral deformities.

Acknowledgements

This work was funded by grant AGL2005-02478 from the Ministry of Education and Culture (MEC) of the Spanish Government. IF was supported by a Portuguese post-doctoral fellowship (SFRH/BPD/82049/2011).

Reference list:

Bustin S, Benes V, Garson JA, Hellemans J, Huggett J, Kubista M, Mueller R, Nolan T, Pfaffl M, Shipley G, Vandesompele J, Wittwer CT (2009) The MIQE guidelines: Minimum information for publication of quantitative real-time PCR experiments. Clin Chem 55: 611–622.

Fernández I, Lopez-Joven C, Andree KB, Roque A, Gisbert E (2015) Dietary vitamin A supplementation in Senegalese sole (*Solea senegalensis*) early juveniles enhance their immunocompetence against induced bacterial infection: new insights on VA immune system-related underlying pathways. Fish Shellfish Immunol 46: 703-709.

Gavaia PJ, Dinis MT, Cancela ML (2002) Osteological development and abnormalities of the vertebral column and caudal skeleton in larval and juvenile stages of hatchery-reared Senegalese sole (*Solea senegalensis*). Aquaculture 211: 305–323.

Infante C, Matsuoka MP, Asensio E, Cañavate JP, Reith M, Manchado M (2008) Selection of housekeeping genes for gene expression studies in larvae from flatfish using real-time PCR. BMC Mol Biol 9**:** 28.

Okada N, Takagi Y, Seikai T, Tanaka M, Tagawa M (2001) Asymmetrical development of bones and soft tissues during eye migration of metamorphosing Japanese flounder, *Paralichthys olivaceus*. Cell Tissue Res 304: 59–66.

Pfaffl MW (2001) A new mathematical model for relative quantification in real-time RT-PCR. Nucleic Acids Res 29:e45.

Richard N, Fernández I, Wulff T, Hamre K, Cancela ML, Conceição LEC, Gavaia PJ (2014) Dietary supplementation with vitamin K affects transcriptome and proteome of Senegalese sole, improving larval performance and quality. Mar Biotechnol 16: 522-537.

Wagemans F, Vandewalle P (2001) Development of the bony skull in common sole: brief survey of morpho-functional aspects of ossification sequence. J Fish Biol 59: 1350–1369.

Table I. Gene name, accession numbers (GenBank), primers and Taqman® probes used for relative quantification of gene expression during Senegalese sole (*Solea senegalensis*) ontogenic development and dietary vitamin A nutritional imbalance during *Artemia* feeding phase.

*GeneBank; **Efficiency (2=100%)

Gene name - ***abbreviation***	Accession number*	Component	5' to 3' nucleotide sequences	E**	Expected amplicon size (bp)
ubiquitin - ubq	AB291588	Forward Reverse Probe	GCCCAGAAATATAACTGCGACAAG TGACAGCACGTGGATGCA ACTTGCGGCATATCAT	1.93	70
retinoic acid receptor alpha - rarα	AB668026	Forward Reverse Probe	GAAGAAGAAGGACGAGAAGAAGCA TGTCTATCATCTGCTCCGTGTCT CAGGACGTAGCTCTCC	1.97	77
retinoic X receptor alpha - rxrα	AB668024	Forward Reverse Probe	CTCATCGTTCCATAGCCGTTAAAGA GCTGTTGCGGTGAACGT TCGCCAACAGAATCC	2.11	68
thyroid hormone receptor alpha a - trαA	AB366000	Forward Reverse Probe	CCGCCTCATTGTCCTGTGA GGACATTGGCTCGGTTTAACCT TTGGCCGCTGGACCAC	1.93	61
thyroid hormone receptor alpha b - trαB	AB444623	Forward Reverse Probe	GAAGCTGGTGCTAAACGGTAGAT CCTCCATCCTTCCCCTACAAAA ACGATGGCCCTTCCCC	1.86	63
thyroid hormone receptor beta - trβ	AB366001	Forward Reverse Probe	CAGAAGCGGAAGTTCCTGAGT TTTGTTTCCTTCAGGTGTGTTTGC ACGCATGACCAATATC	1.89	96
thyriod stimulating hormone beta - tshb	AB297482	Forward Reverse Probe	GAACCAGTGCGGACAGAGTA CAGGAAAAGGGTAGATACGTGTGA AAGTGCAGCAAACCAG	1.89	60
thyroglobulin -tg	AB297481	Forward Reverse Probe	GACCGCCGCCTCTCT TCCTGACGAAGCTGGACATG CTCGCCGTGATGACCT	1.96	52
retinol binding protein -rbp	FF290795	Forward Reverse Probe	CCAGTAAGCAGATCTCCCTCTTCT TCCCGTCATATCACTGGTCTGA CCATCGCCTGGTCCTC	1.89	76
bone Gla protein - bgp	AY823525	Forward Reverse Probe	TCGCTGCCTACACCACCTA GATGAACAACGGTTTGGTGCTAAAA CTATGGACCAATTCCC	2.15	60

*GeneBank; **Efficiency (2=100%)

Figure captures:

Figure 1. Representation of the different steps of the chondral and intramembranous development of skeletal structures from the cranial region of Senegalese sole (*Solea senegalensis*) along development. The age (in days post hatch, dph) or the total length (average ± SD in mm) at which each skeletal structure appeared is depicted. *White bar*, structure not present; *Grey-white squares bar*, cartilage anlagen present; *Grey-white vertical lines bar*, inferred onset of ossification; *Grey bar*, onset of ossification; *Black bar*, advanced ossification. A total of 800 specimens were analyzed (10 per sampling time). *An*, anguloarticular; *Cb*, ceratobranchials; *Clt*, cleithrum; *Mc/Dent*, Meckel cartilage/Dentary; *Ectp*, ectopterygoid; *Epot*, epioccipital; *Eth*, ethmoid; *Exoc*, exoccipital; *F*, frontal bone; *H*, hyoid *Hm*, hyomandibular; *Ih*, interhyal; *Le*, lateral ethmoid; *Max*, maxillary; *Methm*, mesethmoid; *Pa*, parietal; *Par*, parasphenoid; *Pm*, pre-maxila; *Po*, preopercular; *Ptot*, pterotic; *Q*, quadrate; *Sc*, supraorbital canal bones; *Soc*, supraoccipital; *Sph*, sphenoid; *Spot*, sphenotic.

Figure 2. Representation of the different steps of the chondral and intramembranous development of skeletal structures from the trunk region of Senegalese sole (*Solea senegalensis*) along development. The age (in days post hatch, dph) or the total length (average ± SD in mm) at which each skeletal structure appeared is depicted. *White bar*, structure not present; *Grey-white squares bar*, cartilage anlagen present; *Grey-white vertical lines bar*, inferred onset of ossification; *Grey bar*, onset of ossification; *Black bar*, advanced ossification. A total of 800 specimens were analyzed (10 per sampling time). *Av*, abdominal vertebrae; *Ce*, cephalic vertebrae; *Cv*, caudal vertebrae; *Dp*, dorsal pterigophores; *Dr*, dorsal rays; *Hs*, haemal spines; *Mhs*, modified haemal spines; *Mns*, modified neural spine; *Ns*, neural spines; *Pcf*, pectoral fin; *Pp*, parapophysis; *PU-1*, preural vertebra 1; *PU-2*, preural vertebra 2; *Pvf*, pelvic fin; *Ur*, urostyle; *Vp*, ventral pterigophores; *Vr*, ventral rays.

Figure 3. Representation of the different steps of the chondral and intramembranous development of skeletal structures from the caudal fin of Senegalese sole (*Solea senegalensis*) along development. The age (in days post hatch, dph) or the total length (average ± SD in mm) at which each skeletal structure appeared is depicted. *White bar*, structure not present; *Grey-white squares bar*, cartilage anlagen present; *Grey-white vertical lines bar*, inferred onset of ossification; *Grey bar*, onset of ossification; *Black bar*, advanced ossification. A total of 800 specimens were analyzed (10 per sampling time). *Ep*, epural; *H1*, hypural 1; *H2*, hypural 2; *H3*, hypural 3; *H4*, hypural 4; *H5*, hypural 5; *Phy*, Parahypural; *Mhs*, modified haemal spines; *Mns*, modified neural spine; *Fr*, fin rays.

Figure 4. Schematic representation of the developmental stage (pre-, pro- and post-metamorphosis) at which each skeletal structure from Senegalese sole (*Solea senegalensis*) showed an advanced ossification. Skeletal structures were categorized in light grey, structures showing an advanced ossification at pre-metamorphosis; grey, structures showing an advanced ossification at pro-metamorphosis, and black, structures showing an advanced ossification at post-metamorphosis. *An*, anguloarticular; *Av*, abdominal vertebrae; *Bop*, basioccipital; *Cb*, ceratobranchials; *Ce*, cephalic vertebrae; *Clt*, cleithrum; *Cv*, caudal vertebrae; *Dent*, dentary; *Dp*, dorsal pterigophores; *Dr*, dorsal rays; *Ectp*, ectopterygoid; *Ep*, epural; *Epot*, epioccipital; *Exoc*, exoccipital; *F*, frontal bone; *Fr*, fin rays; *H*, hyoid; *H1*, hypural 1; *H2*, hypural 2; *H3*, hypural 3; *H4*, hypural 4; *H5*, hypural 5; *Hm*, hyomandibular; *Hs*, haemal spines; *Ih*, interhyal; *Le*, lateral ethmoid; *Max*, maxillary; *Methm*, mesethmoid; *Mhs*, modified haemal spines; *Mns*, modified neural spine; *Ns*, neural spines; *Pa*, parietal; *Pcf*, pectoral fin; *Phy*, Parahypural; *Pm*, pre-maxila; *Po*, preopercular; *Pp*, parapophysis; *Ptot*, pterotic; *PU-1*, preural vertebra 1; *PU-2*, preural vertebra 2; *Pvf*, pelvic fin; *Q*, quadrate; *Sc*, supraorbital canal bones; *Soc*, supraoccipital; *Sph*, sphenoid; *Spot*, sphenotic; *Ur*, urostyle; *Vp*, ventral pterigophores; *Vr*, ventral rays.

Figure 5. Ontogenetic gene expression patterns along Senegalese sole (*Solea senegalensis*) development. Gene expression measured as the mean expression ratio of the target gene with respect to the house-keeping gene *Ubquitin* (*Ubq*) at each sample time and compared with a reference sample. Reference sample was 9 dph and set to 1. *rarα*, retinoic acid receptor α; *rxrα*, retinoid X receptor α; *rbp*, retinol binding protein; *trαa*, thyroid hormone receptor α a; *trαb*, thyroid hormone receptor α b; *trβ*, thyroid hormone receptor β; *tshβ*, thyroid stimulating hormone β; *tg*, thyroglobulin; *bgp*, bone Gla protein. Light shadowing represents pre- (*no shadowing*), pro- (*light grey shadowing*) and/or post-metamorphosis (*grey shadowing*). Different letters denote significant differences of the global gene expression (ANOVA, $P < 0.05$; $n = 3$).

Figure 6. Relative gene expression from Senegalese sole (*Solea senegalensis*) specimens fed with Control or vitamin A enriched *Artemia* at 10 (a) and 15 (b) days post hatch (dph). Gene expression was measured as the mean expression ratio of the target gene with respect to the house-keeping gene *Ubquitin* (*Ubq*) at each sample time and compared with that of one Control fish (Reference sample and set to 1). *rarα*, retinoic acid receptor α; *rxrα*, retinoid X receptor α; *rbp*, retinol binding protein; *trαa*, thyroid hormone receptor α a; *trαb*, thyroid hormone receptor α b; *trβ*, thyroid hormone receptor β; *tshβ*, thyroid stimulating hormone β; *tg*, thyroglobulin; *bgp*, bone Gla protein. *Whyte bars*, gene expression mean value in soles from Control group; *black bars*, gene expression mean value in soles from VA group; *nd*, gene expression non detected. Asterisks denote significant differences among experimental groups (Student T-test, $P < 0.05$; $n = 3$).

Figure 7. Relative gene expression from Senegalese sole (*Solea senegalensis*) specimens fed with Control or vitamin A enriched *Artemia* at 30 (a) and 41 (b) days post hatch (dph). Gene expression was measured as the mean expression ratio of the target gene with respect to the house-keeping gene *Ubquitin* (*Ubq*) at each sample time and

compared with that of one Control fish (Reference sample and set to 1). *rarα*, retinoic acid receptor α; *rxrα*, retinoid X receptor α; *rbp*, retinol binding protein; *trαa*, thyroid hormone receptor α a; *trαb*, thyroid hormone receptor α b; *trβ*, thyroid hormone receptor β; *tshβ*, thyroid stimulating hormone β; *tg*, thyroglobulin; *bgp*, bone Gla protein. *Whyte bars*, gene expression mean value in soles from Control group; *black bars*, gene expression mean value in soles from VA group. Asterisks denote significant differences among experimental groups (Student T-test, $P < 0.05$; $n = 3$).

Supplementary Figure 1. Double staining of Senegalese sole (*Solea senegalensis*) specimens along larval development showing ossified skeletal elements at 5, 9 13, and 45 days post-hatch (dph). (a) Senegalese sole at 5 dph showing the Meckel's cartilage, anguloarticular, hyoid, quadrate, interhyal, hyomandibular, ethmoid and the pectoral fin in a cartilaginous stage; while cleithrum structure was already revealed with an incipient ossification. (b) Senegalese sole at 9 dph with ossified maxillary, pre-maxila, ectopterygoid, preopercular, anguloarticular, hyoid, quadrate, interhyal, hyomandibular, ethmoid and the parasphenoid, and incipient ossification of exoccipital from the cranial region as well as the neural spines from the axial skeleton. (c) Senegalese sole at 13 dph exhibiting first signs of ossification of the frontal, supraoccipital, epioccipital, pterotic and sphenotic, but advanced one of the exoccipital in the cranial region; an advanced ossification in the different structures composing the whole vertebral column (vertebrae, neural and haemal spines); and an incipient mineralization of the urostyle and the elements forming the caudal fin (fin rays, hypurals, parhypural, modified spines and epural). (d) Senegalese sole at 45 dph with fully ossified skeleton. Scale bar = 1 mm.

Figure 1

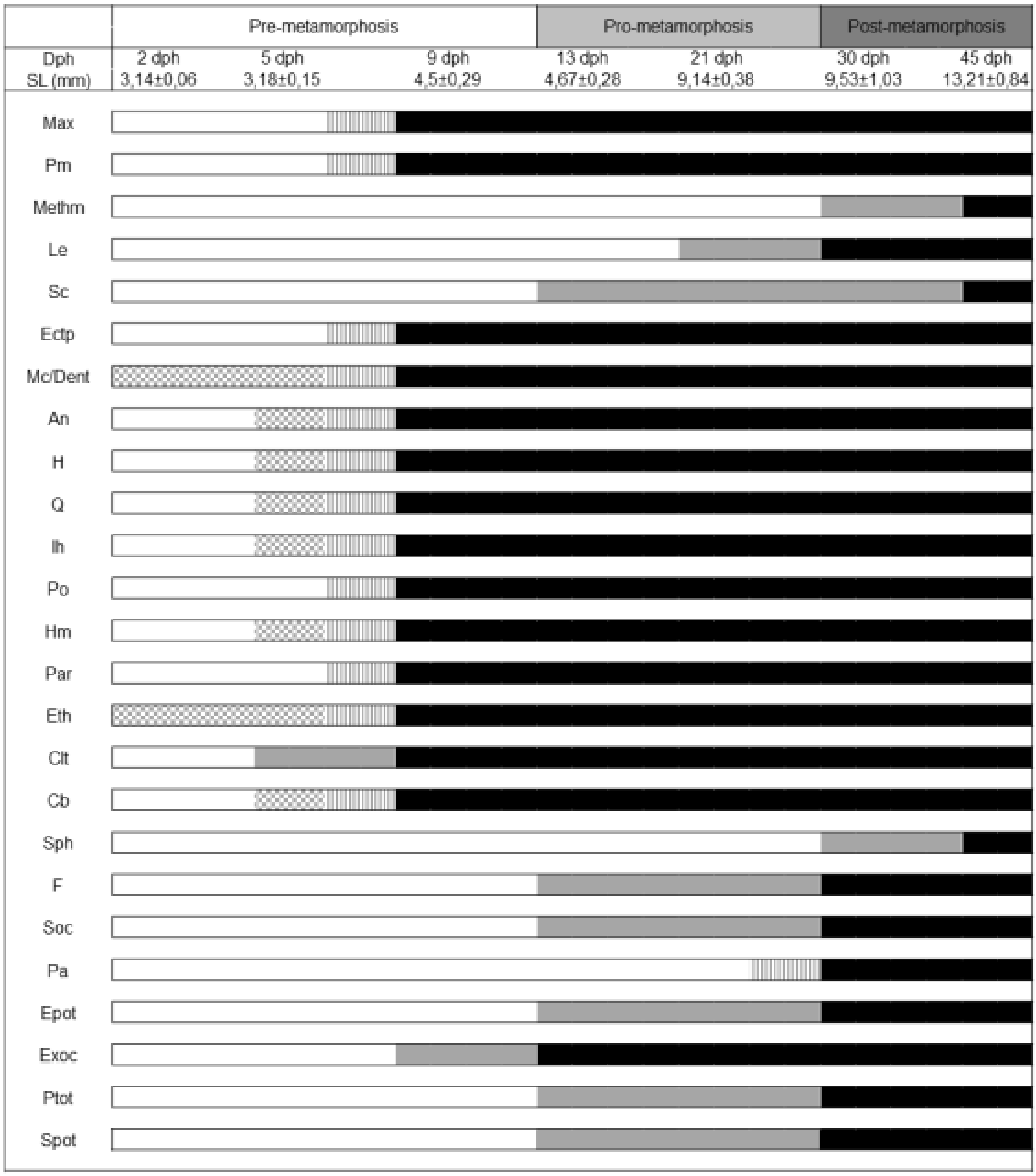
Pre-metamorphosis
Pro-metamorphosis
Post-metamorphosis
Dph
SL (mm)
2 dph
3,14±0,06
5 dph
3,18±0,15
9 dph
4,5±0,29
13 dph
4,67±0,28
21 dph
9,14±0,38
30 dph
9,53±1,03
45 dph
13,21±0,84
Max
Pm
Methm
Le
Sc
Ectp
Mc/Dent
An
H
Q
Ih
Po
Hm
Par
Eth
Clt
Cb
Sph
F
Soc
Pa
Epot
Exoc
Ptot
Spot

Figure 2

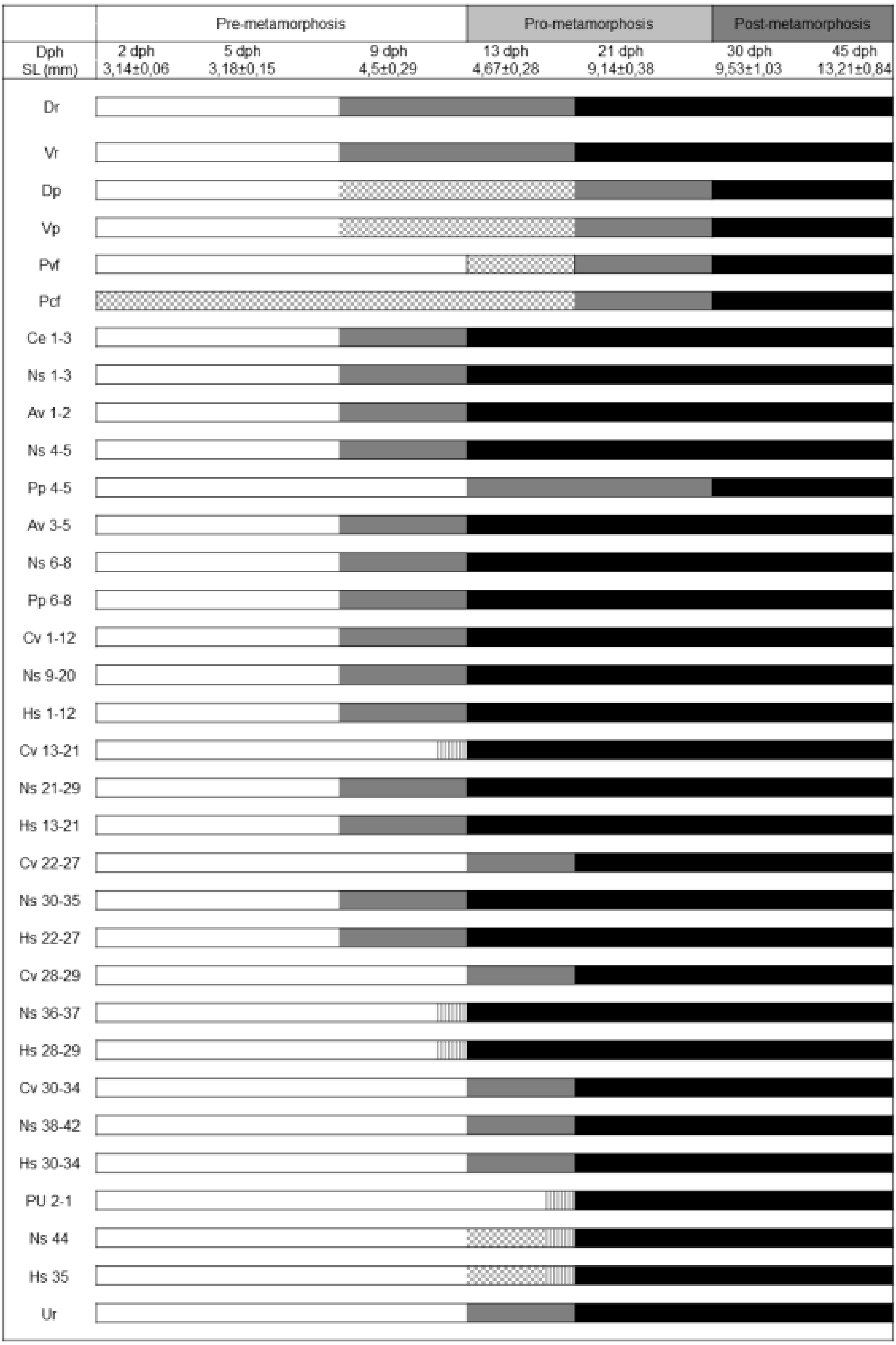
Pre-metamorphosis
Pro-metamorphosis
Post-metamorphosis
Dph
SL (mm)
2 dph
3,14±0,06
5 dph
3,18±0,15
9 dph
4,5±0,29
13 dph
4,67±0,28
21 dph
9,14±0,38
30 dph
9,53±1,03
45 dph
13,21±0,84
Dr
Vr
Dp
Vp
Pvf
Pcf
Ce 1-3
Ns 1-3
Av 1-2
Ns 4-5
Pp 4-5
Av 3-5
Ns 6-8
Pp 6-8
Cv 1-12
Ns 9-20
Hs 1-12
Cv 13-21
Ns 21-29
Hs 13-21
Cv 22-27
Ns 30-35
Hs 22-27
Cv 28-29
Ns 36-37
Hs 28-29
Cv 30-34
Ns 38-42
Hs 30-34
PU 2-1
Ns 44
Hs 35
Ur

Figure 3

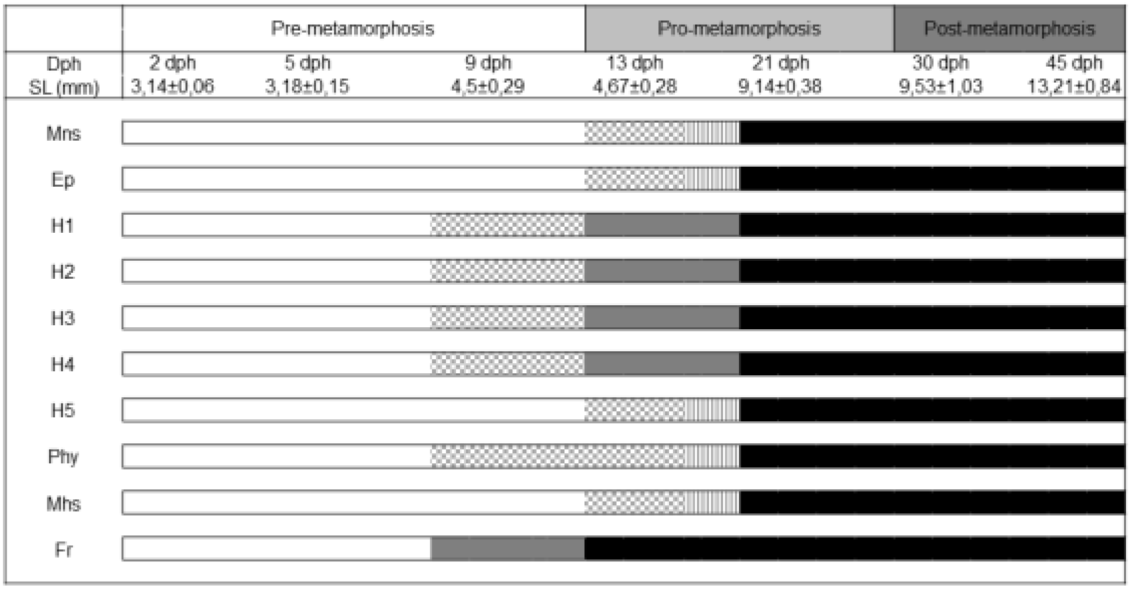
Pre-metamorphosis
Pro-metamorphosis
Post-metamorphosis
Dph
SL (mm)
2 dph
3,14±0,06
5 dph
3,18±0,15
9 dph
4,5±0,29
13 dph
4,67±0,28
21 dph
9,14±0,38
30 dph
9,53±1,03
45 dph
13,21±0,84
Mns
Ep
H1
H2
H3
H4
H5
Phy
Mhs
Fr

Figure 4

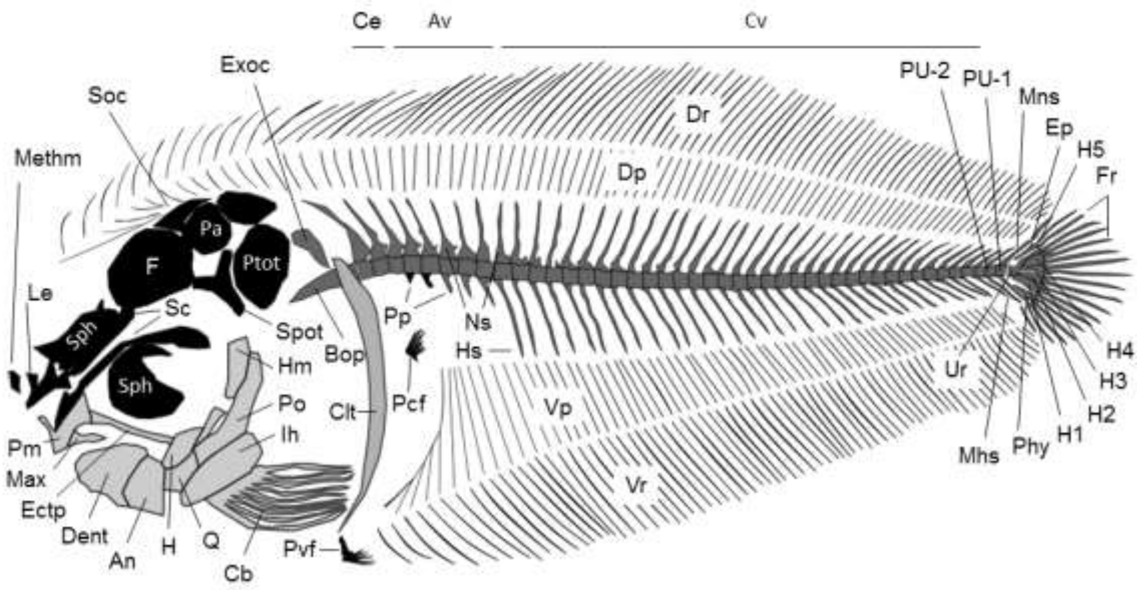
Ce
Av
Cv
Exoc
Soc
Methm
PU-2
PU-1
Mns
Ep
H5
Fr
Dr
Dp
Pa
F
Ptot
Le
Sc
Spot
Sph
Bop
Pp
Ns
Hs
Hm
Sph
Po
Ih
Clt
Pcf
Vp
Ur
H4
H3
H2
H1
Phy
Mhs
Pm
Max
Ectp
Dent
An
H
Q
Cb
Pvf
Vr

Figure 5

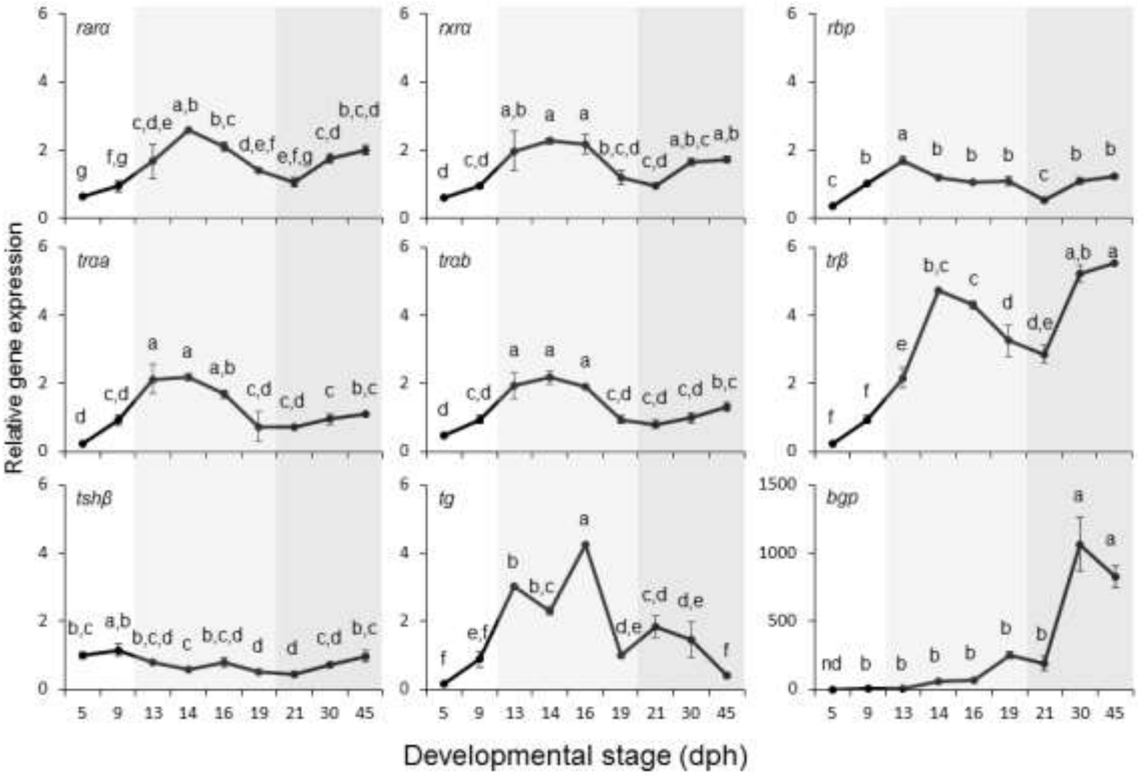

rarα
rxrα
rbp
trαa
trαb
trβ
tshβ
tg
bgp
Relative gene expression
5 9 13 14 16 19 21 30 45
Developmental stage (dph)

Figure 6

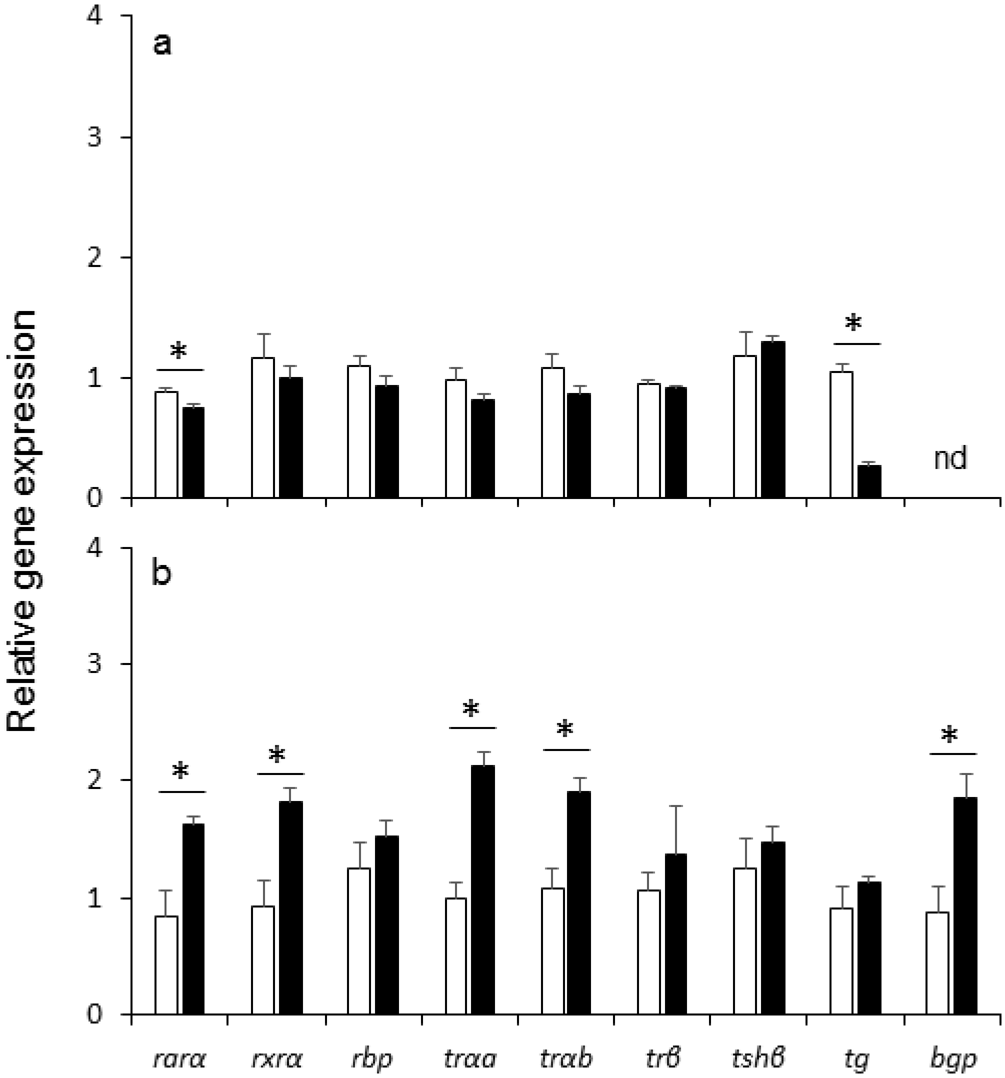
a
b
Relative gene expression
0
1
2
3
4
nd
rarα
rxrα
rbp
trαa
trαb
trβ
tshβ
tg
bgp

Figure 7

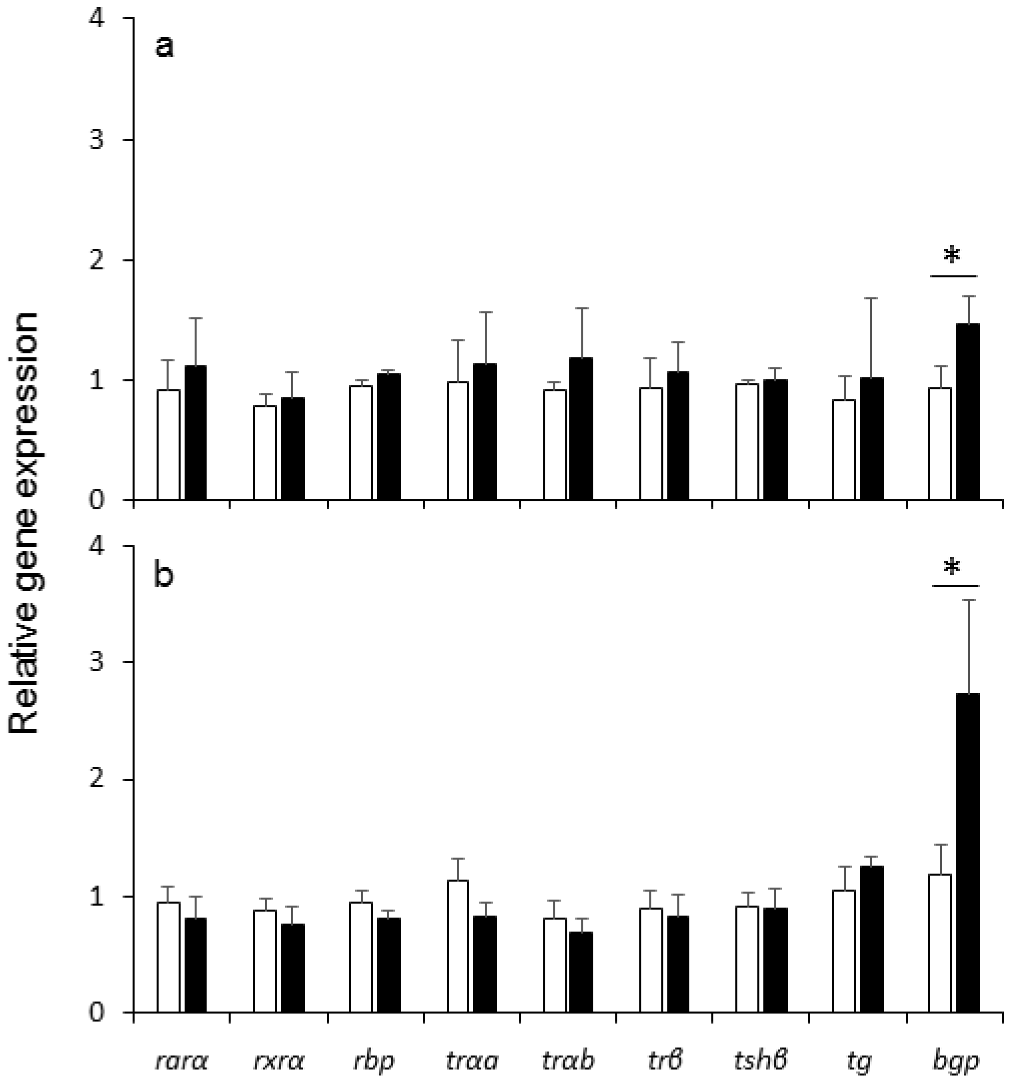
a
b
Relative gene expression
0
1
2
3
4
*
rarα
rxrα
rbp
trαa
trαb
trβ
tshβ
tg
bgp